Acta Mech. Sin. (2011) 27(6):967–976
DOI 10.1007/s10409-011-0514-0

RESEARCH PAPER

Vibration of quadrilateral embedded multilayered graphene sheets based on nonlocal continuum models using the Galerkin method

Babaei H. · Shahidi A.R.

Received: 13 February 2011 / Revised: 27 March 2011 / Accepted: 8 June 2011

Abstract Free vibration analysis of quadrilateral multilayered graphene sheets (MLGS) embedded in polymer matrix is carried out employing nonlocal continuum mechanics. The principle of virtual work is employed to derive the equations of motion. The Galerkin method in conjunction with the natural coordinates of the nanoplate is used as a basis for the analysis. The dependence of small scale effect on thickness, elastic modulus, polymer matrix stiffness and interaction coefficient between two adjacent sheets is illustrated. The non-dimensional natural frequencies of skew, rhombic, trapezoidal and rectangular MLGS are obtained with various geometrical parameters and mode numbers taken into account, and for each case the effects of the small length scale are investigated.

Keywords Small scale · Free vibration · Quadrilateral multilayered graphene sheet · Polymer matrix · Nonlocal elasticity theory

1 Introduction

Much research has been carried out on carbon nanotubes since their invention in 1991 by Ijima [1] and nanostructured elements have attracted a great deal of attention in scientific community due to their superior properties. Understanding the vibration behavior of nanostructures is an important issue from design perspective of many NEMS devices like oscillators, clocks and sensor devices. In structures with small dimensions, long-range inter-atomic and inter-molecular cohesive forces can not be neglected because they strongly affect the static and dynamic properties [2, 3]. To use graphene sheets suitably as MEMS/NEMS component, their vibration response with small scale effects should be studied.

Owing to their discrete structure, atomistic methods such as molecular dynamic simulations, density functional theory, etc. are more appropriate for accurate mechanical analyses of nanostructures. As controlled experiments in nano scale are difficult and molecular dynamic simulations are computationally expensive, theoretical modeling of nanostructures would be an important approach as long as approximate analysis of nanostructures is concerned [4]. Although classical continuum elasticity is a scale-free theory and can not foretell the size effects, however, continuum modeling of nanostructures has gained ever-broaden attention. Using local theory for the small size analysis leads to over-predicting results. To predict micro/nano structures correctly, it is necessary to consider the small scale effects. Some size-dependent continuum theories which take small scale effects into consideration are couple stress elasticity theory [5], strain gradient theory [6], and modified couple stress theory [7]. Besides the above-mentioned models, continuum models with surface stress effects can successfully predict mechanical behaviors of plates at nano scales [8, 9]. However, the nonlocal elasticity theory initiated by Eringen [10] is the most common continuum theory used for analyzing the small-scale structures. In order to capture the small scale effects in nonlocal continuum theory, it is assumed that the stress at a point depends on the strain at all points in the domain. This is contrary to the classical (local) continuum theory in which it is assumed that the stress at a point is just a function of the strain at that point. So, the nonlocal theory contains information about long range interactions between atoms and at internal scale length. Besides the nonlocal continuum theory based models are physically reasonable from the atomistic viewpoint of lattice dynamics and molecular dynamics (MD) simulations [11].

Babaei H.(✉) · Shahidi A.R.
Department of Mechanical Engineering,
Isfahan University of Technology,
Isfahan 8415683111, Iran
e-mail: h.babaei@me.iut.ac.ir

A great deal of attention in the literature has been focused on static, dynamic and stability analysis of micro/nano structures, including analysis of nanobeams [12], nanorods [13], circular nanoplates [14], rectangular nanoplates [15, 16], nanorings [17], and carbon nanotubes (CNTs) [18–21]. Majority of the studies on buckling and vibration of nanoplates are focused on single-layered (SLGS) and multilayered graphene sheets (MLGS). Graphene is a new class of two-dimensional carbon nanostructure which holds great promise for vast applications in many technological fields. Reports related to its applications as strain sensor, mass and pressure sensors, atomic dust detectors, enhancer of surface image resolution are observed [22]. Therefore the attention is attracted to the research of graphene in the field of physics, engineering and material science.

An investigation of the free vibration of arbitrary quadrilateral multilayered graphene sheets embedded in elastic polymer matrix is presented in this paper using nonlocal plate theory with focus laid on the small scale effects and number of layers. The small scale effects are taken into consideration using the nonlocal continuum mechanics. The nonlocal governing equations are derived using the principle of virtual work. The analysis is carried out on the basis of the Galerkin method. Natural coordinates in conjunction with the Galerkin method is used to provide a single superelement which represents the whole plate. The non-dimensional natural frequencies of skew, rhombic, trapezoidal and rectangular nanoplates are obtained with various geometrical parameters, mode numbers and scale coefficients taken into account. The small-scale effects on the natural frequencies of quadrilateral graphene sheets considering various parameters are examined. It is anticipated that the results of the present work would be useful for designing NEMS/MEMS devices using quadrilateral graphene sheets.

2 Formulation

2.1 Single layered nanoplates

The coordinate system used for the nanoplate is shown in Fig. 1.

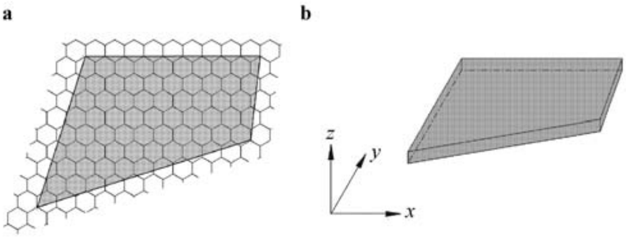

Fig. 1 Model of quadrilateral single layered graphene sheet. **a** Discrete model; **b** Continuum model

Following stress resultants are used in the present formulation

$$\begin{aligned} N_{xx} &= \int_{-h/2}^{h/2} \sigma_{xx}\mathrm{d}z, \qquad N_{yy} = \int_{-h/2}^{h/2} \sigma_{yy}\mathrm{d}z, \\ N_{xy} &= \int_{-h/2}^{h/2} \sigma_{xy}\mathrm{d}z, \qquad M_{xx} = \int_{-h/2}^{h/2} z\sigma_{xx}\mathrm{d}z, \\ M_{yy} &= \int_{-h/2}^{h/2} z\sigma_{yy}\mathrm{d}z, \qquad M_{xy} = \int_{-h/2}^{h/2} z\sigma_{xy}\mathrm{d}z, \end{aligned} \tag{1}$$

where h denotes the height of the plate.

According to classical plate theory (CLPT), the displacement field can be written as

$$\begin{aligned} u_x &= u(x, y, t) - z\frac{\partial w}{\partial x}, \\ u_y &= v(x, y, t) - z\frac{\partial w}{\partial y}, \\ u_z &= w(x, y, t), \end{aligned} \tag{2}$$

where u, v and w denote displacements in x-, y- and z-directions, respectively. The strains can be expressed as

$$\begin{aligned} \varepsilon_{xx} &= \frac{\partial u}{\partial x} - z\frac{\partial^2 w}{\partial x^2}, \qquad \varepsilon_{yy} = \frac{\partial v}{\partial x} - z\frac{\partial^2 w}{\partial y^2}, \\ \varepsilon_{zz} &= 0, \qquad \varepsilon_{xy} = \frac{1}{2}\left(\frac{\partial u}{\partial y} + \frac{\partial v}{\partial x} - 2z\frac{\partial^2 w}{\partial x \partial y}\right), \\ \varepsilon_{xz} &= 0, \qquad \varepsilon_{yz} = 0. \end{aligned} \tag{3}$$

In traditional local elasticity theories, stress at a point depends only on the strain at that point. While here in nonlocal continuum theory it is assumed that the stress at a point depends on strain at all the points of the continuum. By neglecting the body force using nonlocal elasticity theory [10], stress components for a linear homogenous nonlocal elastic body can be represented by the following differential constitutive relation

$$(1 - \mu\nabla^2)\boldsymbol{\sigma} = \boldsymbol{t}, \tag{4}$$

where

$$\mu = (\alpha l_{\mathrm{e}})^2, \qquad \alpha = e_0 l_{\mathrm{i}}/l_{\mathrm{e}}. \tag{5}$$

Here α is the scale coefficient or nonlocal parameter of the length unit describing the effect of micro and nanoscale on the mechanical behavior that depends on internal characteristic lengths (lattice parameter, granular size, distance between C-C bonds) l_{i} and external characteristic lengths (crack length, wave length) l_{e}. The parameter e_0 is so estimated that the relations of the nonlocal elasticity model could provide satisfactory approximation of atomic dispersion curves of plane waves with respect to those of atomic lattice dynamics. Eringen [10] has used the value of 0.39 for e_0. Wang and Hu [23] used strain gradient method to propose an estimate of value e_0, 0.288. Zhang et al. [24] reported $e_0 = 0.82$ from their buckling analysis of carbon nanotubes via Donnell shell theory and molecular mechanics simulations. Duan et al. [25] reported the value of e_0 ranging from 0–19 for carbon nanotubes with nonlocal Timoshenko beam theory and using molecular dynamics results. Duan and Wang [26] used the value of $e_0 l_i$ ranging from 0–2 nm for bending analysis of circular micro/nanoplates. In Eq. (4), ∇^2 is the Laplacian operator and is expressed as $\nabla^2 = (\partial^2/\partial x^2 + \partial^2/\partial y^2)$ and t is the local stress tensor at a point which is related to strain by generalized Hooke's law

$$\boldsymbol{t} = \boldsymbol{S} : \boldsymbol{\varepsilon}, \tag{6}$$

where $\boldsymbol{S}$ is the fourth order elasticity tensor and ":" denotes the double dot product.

Since the principle of virtual work is independent of constitutive relations this can be applied to derive the equilibrium equations for nonlocal plates. Using the principle of virtual work, the following governing equation can be obtained [27]

$$\frac{\partial N_{xx}}{\partial x} + \frac{\partial N_{xy}}{\partial y} = m_0 \frac{\partial^2 u}{\partial t^2}, \tag{7a}$$

$$\frac{\partial N_{yy}}{\partial y} + \frac{\partial N_{xy}}{\partial x} = m_0 \frac{\partial^2 v}{\partial t^2}, \tag{7b}$$

$$\begin{aligned} &\frac{\partial^2 M_{xx}}{\partial x^2} + 2\frac{\partial^2 M_{xy}}{\partial x \partial y} + \frac{\partial^2 M_{yy}}{\partial y^2} + q + \frac{\partial}{\partial x}\left(N_{xx}\frac{\partial w}{\partial x}\right) \\ &\quad + \frac{\partial}{\partial x}\left(N_{xy}\frac{\partial w}{\partial y}\right) + \frac{\partial}{\partial y}\left(N_{yy}\frac{\partial w}{\partial y}\right) + \frac{\partial}{\partial y}\left(N_{xy}\frac{\partial w}{\partial x}\right) \\ &= m_0 \frac{\partial^2 w}{\partial t^2} - m_2\left(\frac{\partial^4 w}{\partial x^2 \partial t^2} + \frac{\partial^4 w}{\partial y^2 \partial t^2}\right), \end{aligned} \tag{7c}$$

where m_0 and m_2 are mass moments of inertia and are defined as follows

$$m_0 = \int_{-h/2}^{h/2} \rho \mathrm{d}z, \qquad m_2 = \int_{-h/2}^{h/2} \rho h^2 \mathrm{d}z, \tag{8}$$

where ρ denotes the density of the material. Using Eq. (4) the two-dimensional nonlocal constitutive relations can be expressed as

$$\begin{aligned} &\begin{Bmatrix} \sigma_{xx} \\ \sigma_{yy} \\ \sigma_{xy} \end{Bmatrix} - \mu \nabla^2 \begin{Bmatrix} \sigma_{xx} \\ \sigma_{yy} \\ \sigma_{xy} \end{Bmatrix} \\ &\quad = \frac{E}{1-\nu^2} \begin{bmatrix} 1 & \nu & 0 \\ \nu & 1 & 0 \\ 0 & 0 & \frac{1-\nu}{2} \end{bmatrix} \begin{Bmatrix} \varepsilon_{xx} \\ \varepsilon_{yy} \\ \varepsilon_{xy} \end{Bmatrix}, \end{aligned} \tag{9}$$

where E and ν denote elastic modulus and Poisson's ratio, respectively. Using strain displacement relationship Eq. (3), stress–strain relationship Eq. (9) and stress resultants definition Eq. (1), one obtains the following nonlocal constitutive relation based on classical plate's theory in terms of displacements

$$M_{xx} - \mu\left(\frac{\partial^2 M_{xx}}{\partial x^2} + \frac{\partial^2 M_{xx}}{\partial y^2}\right) = -D\left(\frac{\partial^2 w}{\partial x^2} + \nu\frac{\partial^2 w}{\partial y^2}\right), \tag{10a}$$

$$M_{yy} - \mu\left(\frac{\partial^2 M_{yy}}{\partial x^2} + \frac{\partial^2 M_{yy}}{\partial y^2}\right) = -D\left(\frac{\partial^2 w}{\partial y^2} + \nu\frac{\partial^2 w}{\partial x^2}\right), \tag{10b}$$

$$M_{xy} - \mu\left(\frac{\partial^2 M_{xy}}{\partial x^2} + \frac{\partial^2 M_{xy}}{\partial y^2}\right) = -D(1-\nu)\frac{\partial^2 w}{\partial x \partial y}, \tag{10c}$$

where D denotes the bending rigidity defined as

$$D = \frac{Eh^3}{12(1-\nu^2)}. \tag{11}$$

If we let M^* denote the moment sum defined by

$$M^* = \frac{M_{xx} + M_{yy}}{1+\nu}, \tag{12}$$

then using Eqs. (7c), (10) and (12) we obtain the nonlocal governing simultaneous differential equations in terms of displacement and moment sum

$$\begin{aligned} &M^* + D\nabla^2 w - \mu \nabla^2 M^* = 0, \\ &\mu \nabla^4 M^* - \nabla^2 M^* + (\mu \nabla^2 - 1)(A - B) = 0, \end{aligned} \tag{13}$$

where

$$A = m_0 \frac{\partial^2 w}{\partial t^2} - m_2\left(\frac{\partial^4 w}{\partial x^2 \partial t^2} + \frac{\partial^4 w}{\partial y^2 \partial t^2}\right), \tag{14}$$

$$\begin{aligned} B = q &+ \frac{\partial}{\partial x}\left(N_{xx}\frac{\partial w}{\partial x}\right) + \frac{\partial}{\partial x}\left(N_{xy}\frac{\partial w}{\partial y}\right) \\ &+ \frac{\partial}{\partial y}\left(N_{yy}\frac{\partial w}{\partial y}\right) + \frac{\partial}{\partial y}\left(N_{xy}\frac{\partial w}{\partial x}\right). \end{aligned} \tag{15}$$

Note that governing equations given in Eq. (13) will be reduced to that of the classical relation when the nonlocal parameter μ is set to zero.

The transverse displacement and sum moment for free vibration is taken as

$$w(x, y, t) = W(x, t)\mathrm{e}^{\mathrm{i}\omega t}, \qquad M^*(x, y, t) = M(x, t)\mathrm{e}^{\mathrm{i}\omega t}. \tag{16}$$

Substituting Eq. (16) into Eq. (13), one obtains the normalized equations of

$$\begin{aligned} &M + D\nabla^2 W - \mu \nabla^2 M = 0, \\ &\mu \nabla^4 M - \nabla^2 M + (\mu \nabla^2 - 1)(A - B) = 0, \end{aligned} \tag{17}$$

where

$$A = \omega^2 (m_0 W - m_2 \nabla^2 W), \tag{18}$$

$$\begin{aligned} B = q &+ \frac{\partial}{\partial x}\left(N_{xx}\frac{\partial W}{\partial x}\right) + \frac{\partial}{\partial x}\left(N_{xy}\frac{\partial W}{\partial y}\right) \\ &+ \frac{\partial}{\partial y}\left(N_{yy}\frac{\partial W}{\partial y}\right) + \frac{\partial}{\partial y}\left(N_{xy}\frac{\partial W}{\partial x}\right). \end{aligned} \tag{19}$$

2.2 Multilayered nanoplates embedded in polymer matrix

In the previous section, differential equation governing the vibration of single layered graphene sheet is derived. Analysis of multilayered graphene sheets embedded in polymer matrix is more important than single layered graphene sheet from practical point of view. In this section this model is extended to multilayered graphene sheets embedded in polymer matrix. The continuum model representing multilayered graphene sheets are shown in Fig. 2. It can be observed that the 1st (topmost) layer and the n-th layers are interacted by polymer matrix and the adjacent layer. Whereas all other in-between layers are acted by two neighboring sheets. Assuming displacements of the sheets as $w_1, w_2, \cdots, w_n$ for the 1st, 2nd, $\cdots$, n-th sheets, respectively, the effective transverse load for various sheets can be written as follows.

Topmost (1st) layer

$$q_1^{\text{eff}} = q - K_{\text{w}} w_1 + K_{\text{p}}\Big(\frac{\partial^2 w_1}{\partial x^2} + \frac{\partial^2 w_1}{\partial y^2}\Big) - C(w_1 - w_2). \quad \text{(20a)}$$

Bottommost (n-th) layer

$$q_n^{\text{eff}} = q - K_{\text{w}} w_n + K_{\text{p}}\Big(\frac{\partial^2 w_n}{\partial x^2} + \frac{\partial^2 w_n}{\partial y^2}\Big) - C(w_n - w_{n-1}). \quad \text{(20b)}$$

Any in-between (i-th layer where $1 < i < n$) layer

$$q_i^{\text{eff}} = q - C(w_i - w_{i-1}) - C(w_i - w_{i+1}), \quad \text{(20c)}$$

where C, K_{w} and K_{p} denote interaction coefficient between two adjacent sheets (representing van der Walls forces), Winkler and shear modulus of polymer matrix, respectively. Using Eqs. (17) and (20), the governing equation for vibration of n layered graphene sheets embedded in a polymer matrix can be written as n number of coupled differential equations as follows

$$\begin{aligned} &M_1 + D\nabla^2 W_1 - \mu\nabla^2 M_1 = 0,\\ &\mu\nabla^4 M_1 - \nabla^2 M_1 + (\mu\nabla^2 - 1)(A_1 - B_1) = 0,\\ &\vdots\\ &M_i + D\nabla^2 W_i - \mu\nabla^2 M_i = 0, \quad 1 < i < n,\\ &\mu\nabla^4 M_i - \nabla^2 M_i + (\mu\nabla^2 - 1)(A_i - B_i) = 0,\\ &\vdots\\ &M_n + D\nabla^2 W_n - \mu\nabla^2 M_n = 0,\\ &\mu\nabla^4 M_n - \nabla^2 M_n + (\mu\nabla^2 - 1)(A_n - B_n) = 0, \end{aligned} \quad (21)$$

where

$$\begin{aligned} &A_i = \omega^2(m_0 W_i - m_2\nabla^2 W_i),\\ &B_i = q_i^{\text{eff}} + \frac{\partial}{\partial x}\Big(N_{xx}\frac{\partial W_i}{\partial x}\Big) + \frac{\partial}{\partial x}\Big(N_{xy}\frac{\partial W_i}{\partial y}\Big)\\ &\qquad + \frac{\partial}{\partial y}\Big(N_{yy}\frac{\partial W_i}{\partial y}\Big) + \frac{\partial}{\partial y}\Big(N_{xy}\frac{\partial W_i}{\partial x}\Big). \end{aligned} \quad (22)$$

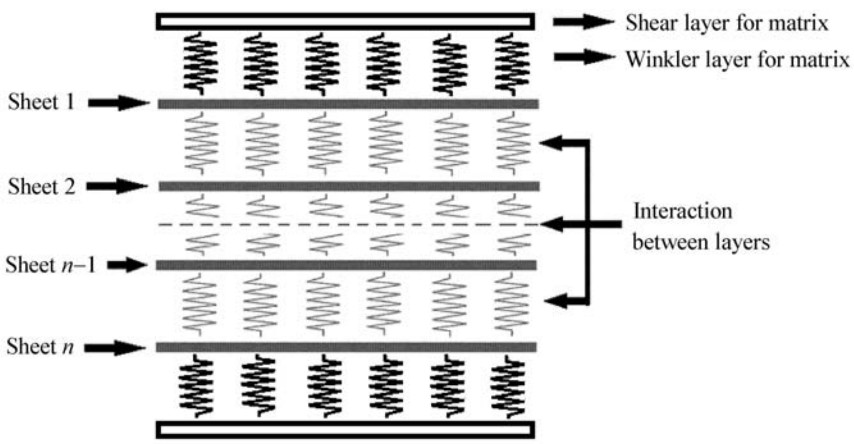

Fig. 2 Continuum model of multilayered graphene sheet embedded in a polymer matrix

3 Solution by Galerkin method

3.1 Geometric definition of the plate

An arbitrary-shaped quadrilateral plate in Cartesian coordinates may be expressed by the mapping of a square plate defined in its natural coordinates with simple boundary equations $\xi = \pm 1$ and $\eta = \pm 1$, as shown in Fig. 3.

For a general quadrilateral plate with straight edge, the displacement transformation from the physical coordinate system to the computational coordinate system is achieved in exact form since the physical coordinate system itself is interpolated exactly. The mapping of the Cartesian coordinate system may be expressed as

$$x(\xi, \eta) = \sum_{i=1}^{N} x_i N_i(\xi, \eta), \qquad y(\xi, \eta) = \sum_{i=1}^{N} y_i N_i(\xi, \eta), \quad (23)$$

where x_i, y_i ($i = 1, 2, \cdots, N$) are the coordinates of N points

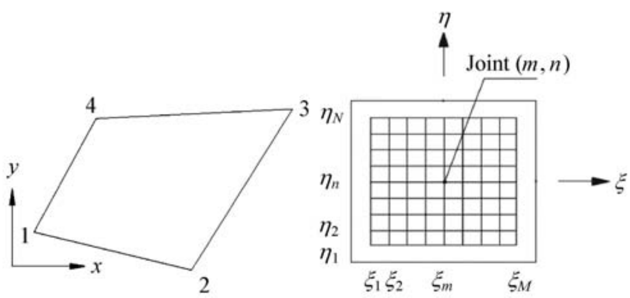

Fig. 3 Mapping of arbitrary quadrilateral plate onto natural coordinates

on the boundary of the quadrilateral region and $N_i(\xi,\eta)$ are the interpolation functions. For an element with straight edges, the interpolation functions are defined by

$$N_i(\xi,\eta) = \frac{1}{4}(1+\xi_i\xi)(1+\eta_i\eta), \tag{24}$$

in which ξ_i and η_i are the natural coordinates of the i-th corner. In order to evaluate the operators ∇^2 and ∇^4, we use the chain rule of differentiation. After some mathematical manipulation, it can be shown that the first-order and second-order derivatives of a function can be expressed by

$$\left\{\begin{array}{c}\dfrac{\partial}{\partial x}\\ \dfrac{\partial}{\partial y}\end{array}\right\} = \boldsymbol{J}_{11}\left\{\begin{array}{c}\dfrac{\partial}{\partial \xi}\\ \dfrac{\partial}{\partial \eta}\end{array}\right\}, \tag{25}$$

$$\left\{\begin{array}{c}\dfrac{\partial^2}{\partial x^2}\\ \dfrac{\partial^2}{\partial y^2}\\ \dfrac{\partial^2}{\partial x\partial y}\end{array}\right\} = \boldsymbol{J}_{22}^{-1}\left(\left\{\begin{array}{c}\dfrac{\partial^2}{\partial \xi^2}\\ \dfrac{\partial^2}{\partial \eta^2}\\ \dfrac{\partial^2}{\partial \xi\partial \eta}\end{array}\right\} - \boldsymbol{J}_{21}\boldsymbol{J}_{11}^{-1}\left\{\begin{array}{c}\dfrac{\partial}{\partial \xi}\\ \dfrac{\partial}{\partial \eta}\end{array}\right\}\right), \tag{26}$$

where $\boldsymbol{J}_{ij}$ are the Jacobian matrixes. These are expressed as follows

$$\boldsymbol{J}_{11} = \begin{bmatrix}\dfrac{\partial x}{\partial \xi} & \dfrac{\partial y}{\partial \xi}\\ \dfrac{\partial x}{\partial \eta} & \dfrac{\partial y}{\partial \eta}\end{bmatrix}, \tag{27}$$

$$\boldsymbol{J}_{21} = \begin{bmatrix}\dfrac{\partial^2 x}{\partial \xi^2} & \dfrac{\partial^2 y}{\partial \xi^2}\\ \dfrac{\partial^2 x}{\partial \eta^2} & \dfrac{\partial^2 y}{\partial \eta^2}\\ \dfrac{\partial^2 x}{\partial \xi\partial\eta} & \dfrac{\partial^2 y}{\partial \xi\partial\eta}\end{bmatrix}, \tag{28}$$

$$\boldsymbol{J}_{22} = \begin{bmatrix}\left(\dfrac{\partial x}{\partial \xi}\right)^2 & \left(\dfrac{\partial y}{\partial \xi}\right)^2 & 2\left(\dfrac{\partial x}{\partial \xi}\right)\left(\dfrac{\partial y}{\partial \xi}\right)\\ \left(\dfrac{\partial x}{\partial \eta}\right)^2 & \left(\dfrac{\partial y}{\partial \eta}\right)^2 & 2\left(\dfrac{\partial x}{\partial \eta}\right)\left(\dfrac{\partial y}{\partial \eta}\right)\\ \left(\dfrac{\partial x}{\partial \xi}\right)\left(\dfrac{\partial x}{\partial \eta}\right) & \left(\dfrac{\partial y}{\partial \xi}\right)\left(\dfrac{\partial y}{\partial \eta}\right) & \left(\dfrac{\partial x}{\partial \xi}\right)\left(\dfrac{\partial y}{\partial \eta}\right)+\left(\dfrac{\partial y}{\partial \xi}\right)\left(\dfrac{\partial x}{\partial \eta}\right)\end{bmatrix}. \tag{29}$$

In this stage, consider the following differential operators

$$\mathrm{R} = \frac{\partial^2}{\partial x^2}, \qquad \mathrm{Q} = \frac{\partial^2}{\partial y^2}. \tag{30}$$

Thus, the fourth-order derivatives can be given in terms of the second-order derivatives [24–28]. The operators ∇^2 and ∇^4 can be expressed by

$$\nabla^2 = \frac{\partial^2}{\partial x^2} + \frac{\partial^2}{\partial y^2} = \mathrm{R} + \mathrm{Q}, \tag{31}$$

$$\begin{aligned}\nabla^4 &= \frac{\partial^4}{\partial x^4} + \frac{\partial^4}{\partial y^4} + 2\frac{\partial^4}{\partial x^2\partial y^2}\\ &= \frac{\partial^2}{\partial x^2}\mathrm{R} + \frac{\partial^2}{\partial y^2}\mathrm{Q} + 2\frac{\partial^2}{\partial x^2}\mathrm{Q}.\end{aligned} \tag{32}$$

3.2 Shape functions

Consider an arbitrary joint (m,n) on a meshed plate which is actually a mapping of the real physical domain, as shown in Fig. 3. If the displacement of the adjoining points in the η-direction is assumed to be zero, then the interpolation function for this point in the ξ-direction will be defined by

$$\psi_m(\xi) = \frac{\prod_{i=0}^{M+1}(\xi-\xi_i)}{\prod_{i=0}^{M+1}(\xi_i-\xi_m)}, \quad i \neq m, \tag{33}$$

and, similarly, the interpolation function for the point (m,n) in the η-direction may be expressed by

$$\psi_n(\eta) = \frac{\prod_{j=0}^{N+1}(\eta-\eta_j)}{\prod_{j=0}^{N+1}(\eta_n-\eta_j)}, \quad j \neq n. \tag{34}$$

Therefore, the interpolation function for point (m,n) in both directions ξ and η are defined by

$$\psi_{mn}(\xi,\eta) = \psi_m(\xi)\psi_n(\eta). \tag{35}$$

The out-of-plane displacement of the plate W is expressed by

$$W = \sum_{m=1}^{M}\sum_{n=1}^{N} A_{mn}\psi_m(\xi)\psi_n(\eta), \tag{36}$$

where M and N are the number of points in the ξ- and η-directions, respectively. If any point (m,n) is assigned an integer k by the relationship

$$k = (m-1) \times N + n, \tag{37}$$

then the flexural displacement W may be defined by

$$W = \sum_{k=1}^{K} a_k \psi_k(\xi, \eta), \tag{38}$$

where $K = M \times N$.

The advantages of expressing W in this way are:

(1) Although a_k or A_{mn} is used as a generalized coordinate, each of quantities is exactly equal to the buckling displacement at point (m, n).

(2) If point (p, q) is introduced as a point support, then the corresponding $a_r = A_{pq}$ can be eliminated in Eqs. (36) and (38). Moreover, for line supports parallel to the ξ- and η-directions, all unknown coefficients a_k for points on the corresponding row or column are eliminated.

Therefore, for a plate with point or line supports, the flexural displacement can be written as

$$W = \sum_{m=1}^{M} \sum_{n=1}^{N} A_{mn} \psi_m(\xi) \psi_n(\eta),$$

$$m \neq p_1, p_2, \cdots, p_R; \qquad n \neq q_1, q_2, \cdots, q_R, \tag{39}$$

where vectors $\boldsymbol{p}$ and $\boldsymbol{q}$ show the coordinates of the R (integer number) restrained joints. An alternative expression for Eq. (39) is

$$W = \sum_{k=1}^{K} a_k \psi_k(\xi, \eta), \quad k \neq k_1, k_2, \cdots, k_R. \tag{40}$$

The moment function M is expressed similarly to the function of W, but without restraints, and thus

$$M = \sum_{k=1}^{K} b_k \psi_k(\xi, \eta), \tag{41}$$

where the coefficients b_k are defined in a manner similar to the coefficients of a_k. When there are no point or line supports, the number of base functions in Eqs. (40) and (41) are equal. However, when some restraint exists, the number of base functions in Eq. (40) is obviously less than those in Eq. (41).

3.3 Solution

Substituting Eqs. (40) and (41) into Eq. (21) and multiplying both sides of the equations by $\psi_i(\xi, \eta)$ and integrating over the whole region yields the following simultaneous linear equations in terms of unknown coefficients $\boldsymbol{a}_i$ and $\boldsymbol{b}_i$

$$\begin{aligned}
&\boldsymbol{K}^{mm}\boldsymbol{b}_1 + D\boldsymbol{K}^{mw}\boldsymbol{a}_1 = 0,\\
&\boldsymbol{K}^{wm}\boldsymbol{b}_1 + \omega^2\boldsymbol{K}_1^{ww}\boldsymbol{a}_1 + \boldsymbol{K}_2^{ww}\boldsymbol{a}_1\\
&\qquad + \boldsymbol{K}_3^{ww}\boldsymbol{a}_1 - \boldsymbol{K}_3^{ww}\boldsymbol{a}_2 = 0,\\
&\vdots\\
&\boldsymbol{K}^{mm}\boldsymbol{b}_i + D\boldsymbol{K}^{mw}\boldsymbol{a}_i = 0, \quad 1 < i < n\\
&\boldsymbol{K}^{wm}\boldsymbol{b}_i + \omega^2\boldsymbol{K}_1^{ww}\boldsymbol{a}_i + 2\boldsymbol{K}_3^{ww}\boldsymbol{a}_i\\
&\qquad - \boldsymbol{K}_3^{ww}\boldsymbol{a}_{i-1} - \boldsymbol{K}_3^{ww}\boldsymbol{a}_{i+1} = 0,\\
&\vdots\\
&\boldsymbol{K}^{mm}\boldsymbol{b}_n + D\boldsymbol{K}^{mw}\boldsymbol{a}_n = 0,\\
&\boldsymbol{K}^{wm}\boldsymbol{b}_n + \omega^2\boldsymbol{K}_1^{ww}\boldsymbol{a}_n + \boldsymbol{K}_2^{ww}\boldsymbol{a}_n\\
&\qquad + \boldsymbol{K}_3^{ww}\boldsymbol{a}_n - \boldsymbol{K}_3^{ww}\boldsymbol{a}_{n-1} = 0.
\end{aligned} \tag{42}$$

Here the components of $\boldsymbol{K}^{mm}$, $\boldsymbol{K}^{mw}$, $\boldsymbol{K}^{wm}$ and $\boldsymbol{K}_i^{ww}$ $(i = 1, 2, 3)$ are given by

$$K_{ij}^{mm} = \int_{-1}^{1}\int_{-1}^{1} \psi_i\psi_j - \mu\psi_i(\nabla^2\psi_j)|J|\mathrm{d}\xi\mathrm{d}\eta, \tag{43a}$$

$$K_{ij}^{mw} = \int_{-1}^{1}\int_{-1}^{1} \psi_i(\nabla^2\psi_j)|J|\mathrm{d}\xi\mathrm{d}\eta, \tag{43b}$$

$$K_{ij}^{wm} = \int_{-1}^{1}\int_{-1}^{1} [\mu\psi_i(\nabla^4\psi_j) - \psi_i(\nabla^2\psi_j)]|J|\mathrm{d}\xi\mathrm{d}\eta, \tag{43c}$$

$$K_{1_{ij}}^{ww} = \int_{-1}^{1}\int_{-1}^{1} \psi_i(\mu\nabla^2 - 1)[m_0\psi_j - m_2(\nabla^2\psi_j)]|J|\mathrm{d}\xi\mathrm{d}\eta, \tag{43d}$$

$$K_{2_{ij}}^{ww} = \int_{-1}^{1}\int_{-1}^{1} \psi_i(\mu\nabla^2 - 1)[K_\mathrm{w}\psi_j - K_p(\nabla^2\psi_j)]|J|\mathrm{d}\xi\mathrm{d}\eta, \tag{43e}$$

$$K_{3_{ij}}^{ww} = \int_{-1}^{1}\int_{-1}^{1} \psi_i(\mu\nabla^2 - 1)(C\psi_j)|J|\mathrm{d}\xi\mathrm{d}\eta. \tag{43f}$$

Considering nontrivial solution of system of Eqs. (42), we have

$$\det\begin{bmatrix}
\gamma_1 & \gamma_2 & 0 & 0 & 0 & 0 & 0 & 0 & 0 & 0\\
\gamma_4 & \gamma_3 & \gamma_6 & 0 & 0 & 0 & 0 & 0 & 0 & 0\\
\vdots & \vdots & \vdots & \ddots & \ddots & \ddots & \vdots & \vdots & \vdots & \vdots\\
0 & 0 & 0 & 0 & 0 & \gamma_1 & \gamma_2 & 0 & 0 & 0\\
0 & 0 & 0 & \gamma_6 & 0 & \gamma_5 & \gamma_3 & \gamma_6 & 0 & 0\\
\vdots & \vdots & \vdots & \vdots & \vdots & \ddots & \ddots & \ddots & \ddots & \vdots\\
0 & 0 & 0 & 0 & 0 & 0 & 0 & 0 & \gamma_1 & \gamma_2\\
0 & 0 & 0 & 0 & 0 & 0 & \gamma_6 & 0 & \gamma_4 & \gamma_3
\end{bmatrix}$$

$$= 0, \tag{44}$$

where

$$\begin{aligned} &\boldsymbol{\gamma}_1 = D\boldsymbol{K}^{mw}, && \boldsymbol{\gamma}_2 = \boldsymbol{K}^{mm}, \\ &\boldsymbol{\gamma}_3 = \boldsymbol{K}^{wm}, && \boldsymbol{\gamma}_4 = \omega^2 \boldsymbol{K}_1^{ww} + \boldsymbol{K}_2^{ww} + \boldsymbol{K}_3^{ww}, \\ &\boldsymbol{\gamma}_5 = \omega^2 \boldsymbol{K}_1^{ww} + 2\boldsymbol{K}_3^{ww}, && \boldsymbol{\gamma}_6 = -\boldsymbol{K}_3^{ww}. \end{aligned} \tag{45}$$

This equation can be solved for ω, for a given number of layers.

4 Results and discussion

To illustrate the small scale or nonlocal effect on the vibration response, we define frequency ratio as follows [29]

$$\text{frequency ratio} = \frac{\text{natural frequency calculated from nonlocal theory}}{\text{natural frequency calculated from local theory}}.$$

For single layered sheet, it was observed that the frequency ratio is independent of the thickness of the sheets [29]. But it can be seen from Eq. (44) that frequency ratio for embedded multilayered plate is dependent on the thickness of the plate. Further in this case, this frequency ratio can be seen to be dependent on even the material properties of graphene. To illustrate the dependence of small scale effect on thickness, elastic modulus, polymer matrix stiffness and interaction coefficient between two adjacent sheets a general simply supported skew shaped embedded multilayered graphene sheet with the following properties [29] is considered. The elastic modulus are taken as $E = 1\,765$ GPa, Poisson's ratios $\nu = 0.3$, thickness of each plate $h = 0.34$ nm, interaction coefficient between two layers $C = 45 \times 10^{18}$ Pa/m, polymer matrix Winkler modulus $K_w = 1.13 \times 10^{18}$ Pa/m, polymer matrix shear modulus $K_p = 1.13$ Pa/m, number of layers is 5, skew angle $\beta = 45°$ (see Fig. 4a) and aspect ratio $L/b = 1$ (see Fig. 4a). The scale coefficients or nonlocal parameter are taken as $e_0 l_i = 2$ nm and the external characteristic lengths are taken as $l_e = 5$ nm. These value are taken because $e_0 l_i$ should be smaller than 2.0 nm for carbon nanotubes as described by Wang and Wang [30]. It should be noted that the value of nonlocal parameter is not exactly known for graphene sheet [22]. Frequency ratio has been plotted against percentage change of h, E, K_w, K_p and C one at a time in Figs. 5 and 6.

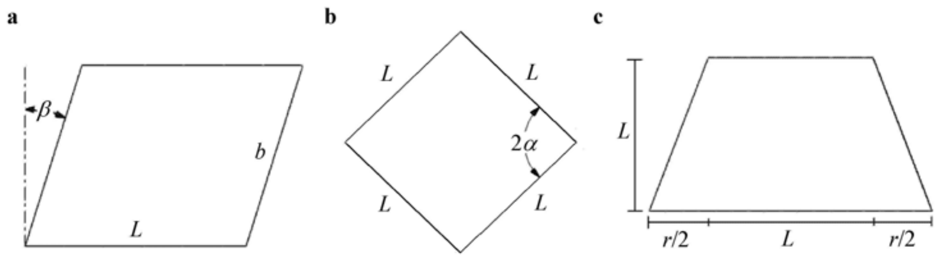

Fig. 4 Various geometry of quadrilateral embedded multilayered graphene sheet. **a** Skew MLGS, **b** Rhombic MLGS; **c** Trapezoidal MLGS

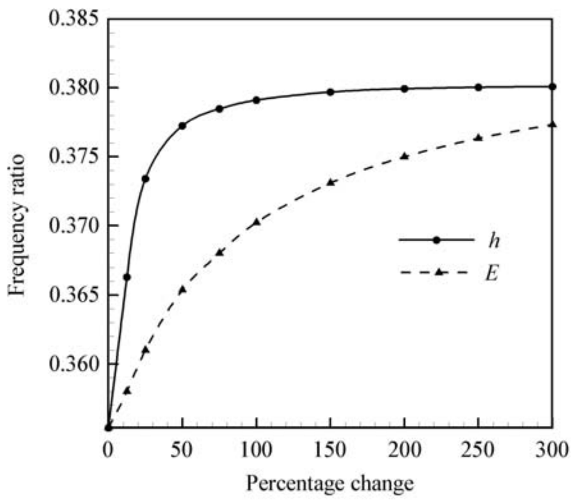

Fig. 5 Variation of frequency ratio of embedded multilayered graphene sheet with percentage change of h and E

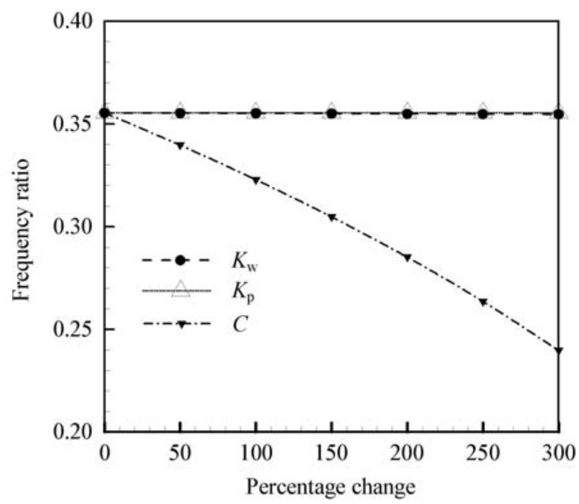

Fig. 6 Variation of frequency ratio of embedded multilayered graphene sheet with percentage change of K_w, K_p and C

It can be seen that nonlocal effect decreases when h increases. This is obvious because the small size effect reduces with increase of MLGS' thickness. Further it is observed that the frequency ratio converges to 0.38 when the percentage change of h is 200 as shown in Fig. 5. Also nonlocal effect decreases as E increases. Figure 6 shows that nonlocal effect is independent of shear and Winkler modulus while it can be seen to be increased with increase in interaction coefficient.

To illustrate the dependence of small scale effect on number of layers, a general simply supported skew multilayered graphene sheet is considered for the same properties as described in the previous section. Four modes of vibration for different nonlocal parameters are considered and frequency ratio is plotted against number of layers in Fig. 7.

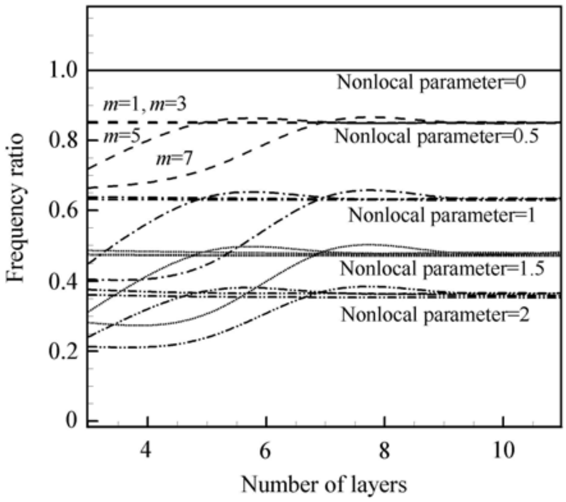

Fig. 7 Variation of frequency ratio with number of layers for various mode numbers (m) and nonlocal parameter

It can be clearly observed that number of layer effect is negligible for lower (first, second and third) modes while it is significant for higher modes. Further it can be observed that the effect of number of layer on small scale effect continues to decrease up to a specific number of layer (e.g. five layers for the fifth mode and seven layers for the seventh mode) and then the frequency ratio converges to certain value corresponding to lower modes.

To illustrate the influence of small length scale on the vibration of general simply supported quadrilateral MLGS, the non-dimensional natural frequency parameters ($\Omega = \omega b^2 \sqrt{\rho}/\pi^2$) is studied for different scale coefficients and geometrical parameters. At first skew MLGS embedded in a polymer matrix is considered. For various nonlocal parameters and aspect ratios of the plates the natural frequencies are plotted in Fig. 8. A value of $\beta = 45°$ is taken for skew angle (see Fig. 4a). This figure shows a profound scale effect for smaller aspect ratios and higher values of nonlocal parameter. From this figure it can also be observed that lower natural frequency is obtained at higher values of nonlocal parameter. Further it can be observed that as the aspect ratios increases, the natural frequency decreases. Natural frequencies for various nonlocal parameters and skew angles of the plate are plotted in Fig. 9. A value of $L/b = 1$ is taken for the aspect ratio. It is observed that the natural frequency increases when the skew angle increases from 0° to 75°.

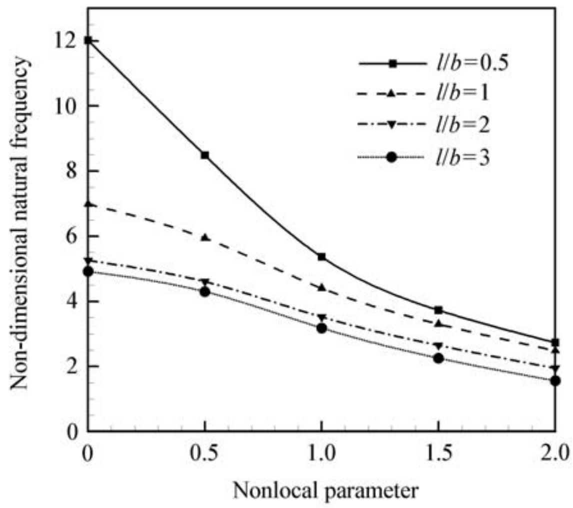

Fig. 8 Variation of non-dimensional natural frequencies of skew embedded multilayered graphene sheet versus nonlocal parameter for different aspect ratios

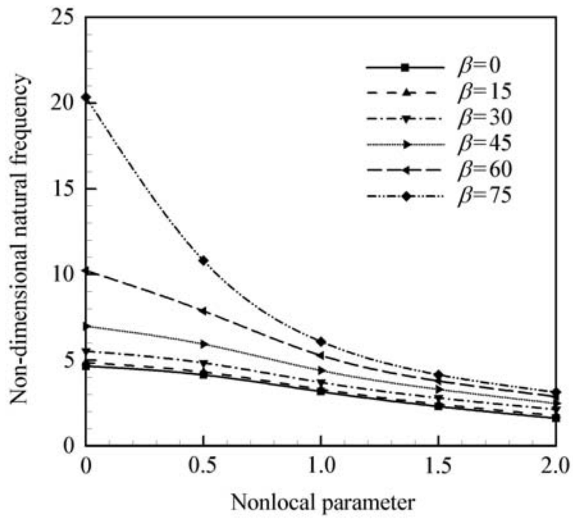

Fig. 9 Variation of non-dimensional natural frequencies of skew embedded multilayered graphene sheet versus nonlocal parameter for different skew angles

Natural frequencies for skew MLGS with higher skew angles (e.g. $\beta = 75°$) are strongly affected by small scale in comparison with skew MLGS with lower skew angles (e.g. $\beta = 0°$).

From Figs. 8 and 9 it is seen that as the value of small scale coefficient increases the value of non-dimensional natural frequency of small-scale plates decreases. Also the effects of aspect ratio and skew angle on the natural frequency decrease when the scale coefficient increases. This phenomenon is attributed to the size effects. At micro/nano level the plate structure can no longer be considered as homogenous but discrete in nature. Hence there is a softening of the plate. Also many experimental evidences show size-dependent mechanical properties when the scale is small enough. Compared with classical plate theories [31] where buckling load do not vary with the scale parameters, the nonlocal plate theories can predict changes of natural frequency induced by the scale effects. Therefore, the classical continuum mechanics fails to capture the nature of size dependent properties.

Next we will illustrate the effect of nonlocal parameter on the natural frequencies of rhombic MLGS.

Figure 10 shows the variation of natural frequency with nonlocal parameter for various values of the rhombic angle (α) (see Fig. 4b) of rhombic MLGS. The range of this angle is 15°–45°. It is observed that the natural frequency decreases when rhombic angle increases from 15° to 45°. Further it is found that the nonlocal effects are more pronounced for higher rhombic angle.

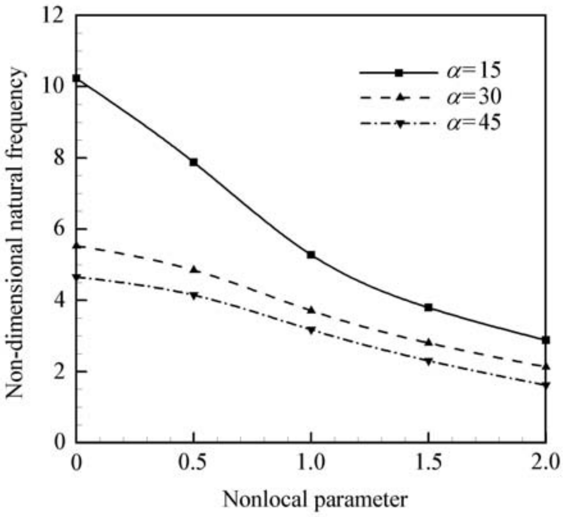

Fig. 10 Variation of non-dimensional natural frequencies of rhombic embedded multilayered graphene sheet versus nonlocal parameter for different rhombic angles

Finally the variation of natural frequency versus scale coefficient for various aspect ratios (r/L) (see Fig. 4c) of trapezoidal MLGS is studied (Fig. 11). The range of variation is r/L = 0–1. It is observed that the natural frequency decreases when the aspect ratio increases from 0 to 1.

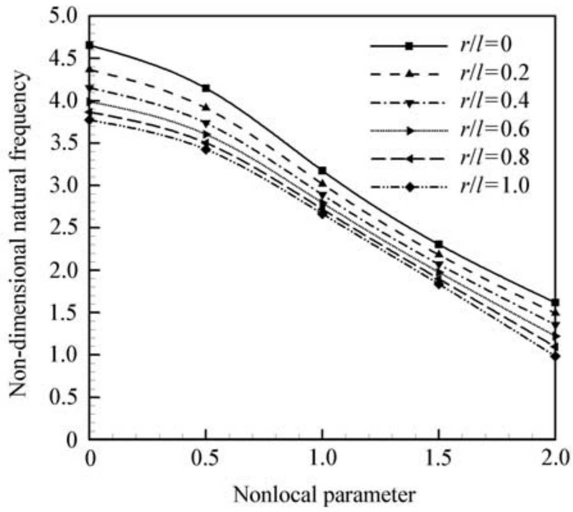

Fig. 11 Variation of non-dimensional natural frequencies of trapezoidal embedded multilayered graphene sheet versus nonlocal parameter for different aspect ratios

5 Conclusion

This study is concentrated on the free vibration analysis of general simply supported quadrilateral MLGS embedded in polymer matrix via nonlocal continuum mechanics. Equations of motion of the plates were derived based on Eringen's differential constitutive equations of nonlocal elasticity. The Galerkin method was introduced as a numerical procedure for the vibration analysis of general simply supported quadrilateral MLGS. The straight-sided quadrilateral domain is mapped onto a square domain in the computational space using a four-node element. The discretizing and programming procedures are straightforward and easy. The dependence of small scale effect on thickness, elastic modulus, polymer matrix stiffness and interaction coefficient between two adjacent sheets was illustrated. It is clearly observed that number of layer effect is negligible for lower (first, second and third) modes while it is significant for higher modes. Further it is found that the effect of the number of layer on small scale effect continues to decrease up to a specific number of layer (e.g. five layers for the fifth mode and seven layers for the seventh mode) and then the frequency ratio converges to certain value corresponding to lower modes. The non-dimensional natural frequencies were obtained for skew, rhombic, rectangular and trapezoidal MLGS embedded in polymer matrix with various geometrical parameters and scale coefficients taken into account, and for each case the significance of the small scale effects was discussed.

References

1 Iijima, S.: Helical microtubules of graphitic carbon. Nature **354**, 56–58 (1991)
2 Wong, E.W, Sheehan, P.E., Lieber, C.M.: Nanobeam mechanics: elasticity, strength, and toughness of nanorods and nanotubes. Science **277**, 1971–1975 (1997)
3 Sorop, T.G., Jongh, de L.J.: Size-dependent anisotropic diamagnetic screening in superconducting Sn nanowires. Physical Review B **75**, 014510 (2007)
4 Murmu, T., Pradhan, S.C.: Buckling of bi-axially compressed orthotropic plates at small scales. Mechanics Research Communications **36**, 933–938 (2009)
5 Zhou, S.J., Li, Z.Q.: Length scales in the static and dynamic torsion of a circular cylindrical micro-bar. Journal of Shandong University of Technology **31**, 401–407 (2001) (in Chinese)
6 Fleck, N.A., Hutchinson, J.W.: Strain gradient plasticity. Advances in Applied Mechanics **33**, 296–358 (1997)
7 Yang, F., Chong, A.C.M., Lam, D.C.C., et al.: Couple stress based strain gradient theory for elasticity. International Journal Solids and Structures **39**, 2731–2743 (2002)
8 Miller, R.E., Shenoy, V.B.: Size-dependent elastic properties of nanosized structural elements. Nanotechnology **11**, 139–147 (2000)
9 Wang, Z.Q., Zhao, Y.P.: Self-instability and bending behaviors of nano plates. Acta Mech. Solida Sinica **22**, 630–643 (2009)
10 Eringen, A.C.: On differential equations of nonlocal elasticity and solutions of screw dislocation and surface waves. Journal of Applied Physics **54**, 4703–4710 (1983)
11 Chen, Y., Lee, J.D., Eskandarian, A.: Atomistic viewpoint of the applicability of microcontinuum theories. Int. J. Solids Struct. **41**, 2085–2097 (2004)
12 Lu, P., Lee, H.P., Lu, C., et al.: Dynamic properties of flexural beams using a nonlocal elasticity model. J. Appl. Phys. **99**, 073510 (2006)
13 Aydogdu, M.: Axial vibration of the nanorods with the nonlocal continuum rod model. Physica E **41**, 861–864 (2009)
14 Duan, W.H., Wang, C.M.: Exact solutions for axisymmetric bending of micro/nanoscale circular plates based on nonlocal plate theory. Nanotechnology **18**, 385704 (2007)
15 Murmu, T., Pradhan, S.C.: Vibration analysis of nano-single-layered graphene sheets embedded in elastic medium based on nonlocal elasticity theory. J. Appl. Phys. **105**, 064319 (2009)
16 Pradhan, S.C., Phadikar, J.K.: Small scale effect on vibration of embedded multilayered graphene sheets based on nonlocal continuum models. Phys. Lett. A. **37**, 1062–1069 (2009)
17 Wang, C.M., Duan, W.H.: Free vibration of nanorings/arches based on nonlocal elasticity. J. Appl. Phys. **104**, 014303 (2008)
18 Reddy, J.N., Pang, S.D.: Nonlocal continuum theories of beams for the analysis of carbon nanotubes. J. Appl. Phys. **103**, 023511 (2008)
19 Murmu, T., Pradhan, S.C.: Buckling analysis of a single-walled carbon nanotube embedded in an elastic medium based on nonlocal elasticity and Timoshenko beam theory and using DQM. Physica E **41**, 1232–1239 (2009)
20 Heireche, H., Tounsi, A., Benzair, A., et al.: Sound wave propagation in single-walled carbon nanotubes. Physica E **40**, 2791–2799 (2008)
21 Wan, L.: Dynamical behaviors of double-walled carbon nanotubes conveying fluid accounting for the role of small length scale. Comput. Mater. Sci. **45**(2), 584–588 (2009)
22 Pradhan, S.C., Murmu, T.: Small scale effect on the buckling of single-layered graphene sheets under biaxial compression via nonlocal continuum mechanics. Computational Materials Science **47**, 268–274 (2009)
23 Wang, L., Hu, H.: Flexural wave propagation in single-walled carbon nanotubes. Physical Review B **71**, 195412 (2005)
24 Zhang, Y.Q., Liu, G.R., Xie, X.Y.: Free transverse vibrations of double-walled carbon nanotubes using a theory of nonlocal elasticity. Physical Review B **71**, 195404 (2005)
25 Duan, W.H., Wang, C.M., Zhang, Y.Y.: Calibration of nonlocal scaling effect parameter for free vibration of carbon nanotubes by molecular dynamics. Journal of Applied Physics **101**, 024305 (2007)
26 Duan, W.H., Wang, C.M.: Exact solutions for axisymmetric bending of micro/nanoscale circular plates based on nonlocal plate theory. Nanotechnology **18**, 385704 (2007)
27 Reddy, J.N.: Mechanics of Laminated Composite Plates, Theory and Analysis, Chemical Rubber Company, Boca Raton, FL (1997)
28 Liew, K.M., Han, J.B.: A four–note differential quadrature method for straight-sided quadrilateral Reissner/Mindlin plates. Commun. Num. Meth. Eng. **13**, 73–81 (1997).
29 Pradhan, S.C., Phadikar, J.K.: Small scale effect on vibration of embedded multilayered graphene sheets based on nonlocal continuum models. Physics Letters A **373**, 1062–1069 (2009)
30 Wang, Q., Wang, C.M.: The constitutive relation and small scale parameter of nonlocal continuum mechanics for modeling carbon nanotubes. Nanotechnology **18**(7), 075702 (2007)
31 Reddy, J.N.: Theory and Analysis of Elastic Plates. Taylor and Francis, Philadelphia, PA. (1999)